Dehalogenation of α-hexachlorocyclohexane by iron sulfide nanoparticles: Study of reaction mechanism with stable carbon isotopes and pH variations

Silviu-Laurentiu Badea, Diana-Ionela Stegarus, Violeta-Carolina Niculescu, Stanica Enache, Amalia Soare, Roxana-Elena Ionete, Didier Gori, Patrick Höhener

Dehalogenation of α-hexachlorocyclohexane by iron sulfide nanoparticles: study of reaction mechanism with stable carbon isotopes and pH variations

Silviu-Laurentiu Badea[1]*, Diana-Ionela Stegarus[1], Violeta-Carolina Niculescu[1], Stanica Enache[1], Amalia Soare[2], Roxana-Elena Ionete[1], Didier Gori[2], Patrick Höhener[2]

[1]National Research and Development Institute for Cryogenic and Isotopic Technologies – ICSI Rm. Vâlcea, 4th Uzinei Street, 240050 Ramnicu Vâlcea, Romania

[2]Environmental Chemistry Laboratory (LCE), Aix-Marseille Université-CNRS UMR 7376, 3 place Victor Hugo - Case 29, 13331 Marseille Cedex 3, France

*corresponding author:

Silviu-Laurentiu Badea

E-mail: silviu.badea@icsi.ro

Phone: +40 250 732744

Fax: +40 250 732746

Abstract

The biodegradation of hexachlorocyclohexanes (HCHs) is known to be accompanied by isotope fractionation of carbon ($^{13}C/^{12}C$), but no systematic studies were performed on abiotic degradation of HCH isomers by iron (II) minerals. In this study, we explored the carbon isotope fractionation of α-HCH during dechlorination by FeS nanoparticles at different pH values. The results of three different experiments showed that the apparent rate constants during dehalogenation of α-HCH by FeS increased with pH. The lowest apparent rate constant value α-HCH during dehalogenation by FeS was 0.009 d^{-1} at pH value of 2.4, while the highest was 1.098 d^{-1} at pH 11.8. α-HCH was completely dechlorinated by FeS only at pH values 9.9 and 11.8, while the corresponding apparent rate constants were 0.253 d^{-1} and 1.098 d^{-1}, respectively. Regardless of the pH used, the 1,2,4-trichlorobenzene (1,2,4-TCB), 1,2-dichlorobenzene (1,2-DCB), and benzene were the dominant degradation products of α-HCH. An enrichment factor (ε_C) of -4.7 ± 1.3 ‰ was obtained for α-HCH using Rayleigh model, which is equivalent to an apparent kinetic isotope effect (AKIEC) value of 1.029 ± 0.008 for dehydrohalogenation, and of 1.014 ± 0.004 for dihaloelimination, respectively. The magnitude of isotope fractionation from this study suggests that abiotic isotope fractionation by FeS must be taken into account in anoxic sediments and aquifers contaminated with HCH isomers, when high concentrations of FeS are present in the above-mentioned anoxic environments.

Keywords:

dehalogenation, HCH, CSIA, FeS, dehydrohalogenation, reductive dechlorination

1. Introduction

The abiotic transformation of emerging and priority pollutants has been less studied compared to biodegradation. This is the case of abiotic reductive dehalogenation, a process that can mimic the anoxic transformation of halogenated contaminants (i.e. chlorinated ethenes, chlorinated ethanes, hexabromocyclododecane (HBCD), etc) in the environment (Wacławek et al., 2019). The contaminants can be abiotically transformed by iron (II) minerals (He et al., 2015) formed either by microbial activity or occurring in nature as part of the site geochemistry. The minerals capable of abiotic contaminant transformation include iron sulfides (mackinawite (FeS), pyrite (FeS_2), greigite (Fe_3S4)) and additional iron (II) minerals such as magnetite (Lee and Batchelor, 2002), green rust (Ayala-Luis et al., 2012), and phyllosilicate clays (biotite (Kriegman-King and Reinhard, 1992) and vermiculite (Bae and Lee, 2012)). Among the most important of these iron (II) minerals is iron sulfide (FeS), a mineral with reductive properties that appears naturally in various anoxic environments (in concentrations often exceeding 10 μmol/g dry weight (Li et al., 2016)), being associated with sulfate-reducing bacteria that grow in anoxic aquifers and sediments. The natural formation of FeS involves two steps. The first step is biotic and consists in HS^- ion generation by sulfate-reducing microorganisms from sulfate, as well in parallel Fe(II) generation from naturally occurring Fe(III) oxyhydroxides by iron-reducing microorganisms. The second step results in the rapid precipitation of poorly crystalline and reactive iron sulfide species. Considering that the accidental pollutions or the unsound disposal practices may lead to the spreading of organohalogen contaminants into environment, those compounds can be transformed, in anoxic sediment and aquifers, by biotic or abiotic processes. Beside biodegradation by various bacteria, the organohalogen contaminants can also be abiotically transformed, in the presence of the reactive iron sulfide species, as electrons are donated from the iron sulfide to the halogenated contaminants (i.e. HCHs, HBCDs, etc).

FeS nanoparticles have also been synthesized under laboratory conditions by various methods and they were used in the elimination of different organohalogen contaminants. Previous studies have reported the capacity of FeS to reductively dehalogenate various halogenated organic pollutants, such as hexachloroethane (Butler and Hayes, 1998), trichloroethylene (Butler et al., 2013; He et al., 2010), γ-hexachlorocyclohexane (γ-HCH) (Liu et al., 2003) and hexabromocyclododecane (HBCD) (Li et al., 2016). (Nie et al., 2020) recently showed that the degradation of trichloroethylene by biotic FeS was six time faster than its degradation by abiotic FeS. The higher reductive activity of the biogenic FeS detected by (Nie et al., 2020) was attributed to a higher monosulfide (HS^- ion) content and to more structural Fe^{2+} on the surface.

Compound specific isotope analysis (CSIA) of carbon isotopes is using the preferential transformation of lighter isotopomers during a biotic or abiotic reaction, therefore leading to an enrichment of heavier isotopes in the residual phase of substrate (Elsner and Imfeld, 2016). In order to relate the change of bulk isotope ratios of chemicals to the extent of the target compound degradation, the Rayleigh model has been extensively used in environmental studies (Julien et al., 2018). The carbon, hydrogen and chlorine based CSIA is currently available for more simple organic contaminants, such as BTEX (Elsner and Imfeld, 2016; Lesser et al., 2008; Vogt et al., 2016) and chlorinated ethenes (Kuder et al., 2013; Marco-Urrea et al., 2011), and these concepts are already applied in the monitoring of contaminated sites (Hunkeler, 2008). Conversely, the concepts and applications of CSIA for larger molecules including chemical classes such as pesticides, flame retardants, and other emerging products are still nascent areas of research and urgently need further development (Elsner and Imfeld, 2016). Hexachlorocyclohexane (HCH) belongs to the organochlorine compounds and its γ-isomer (Lindane) is a globally applied broad-spectrum insecticide (Muller and Kohler, 2004). HCH has been classified as persistent organic pollutant by the Stockholm Convention due to his adverse effects on humans and environment (Wacławek et al., 2019). HCH consists of eight isomers (α-, β-, γ-, δ-, ε-, η-, υ-, and ι-HCH), of

which only the α-HCH is a chiral compound. CSIA has been applied in the past to characterize the biodegradation of HCH isomers using sulfate-reducing bacteria (Badea et al., 2009), fermentative microorganisms (Badea et al., 2011), a Dehalococcoides strain (Liu et al., 2020a), aerobic cultures (Sphingobium spp (Bashir et al., 2013), and Sphingobium indicum Strain B90A (Liu et al., 2019)), some studies involving also multi-element (C-Cl) CSIA (Liu et al., 2020a).

This study aims to investigate the mechanism and pathway of α-HCH dehalogenation by FeS nanoparticles using the carbon isotope fractionation under anoxic conditions, in order to be able to differentiate this process from biotic degradation in the field. To this end, the influence of pH on the degradation rate were included, degradation products were identified and a mass balance of substrate and products was established.

2. Materials and Methods

2.1. Chemicals

$FeSO_4 \cdot 7\ H_2O$ (99% analytical purity) was purchased from Honeywell (Seelze, Germany), while sodium sulfide hydrate (with 65.6 % Na_2S content) was purchased from Sigma–Aldrich (Munich, Germany). α-HCH (99%) and hexachlorobenzene (HCB) (99%), 1,2,4-trichlorbenzene (1,2,4-TCB) (99%), 1,2-dichlorobenzene (1,2-DCB) (99%) and benzene (99%) were obtained from Sigma–Aldrich (Munich, Germany). Anhydrous Na_2SO_4 and hydrochloric acid (HCl) was purchased from Sigma–Aldrich (Munich, Germany). Dichloromethane (DCM) (99.8 %) was purchased from Carl Roth (Karlsruhe, Germany).

2.2. Synthesis of FeS nanoparticles

FeS nanoparticles were synthesized by adding 250 mL solution of 0.2 M Na_2S over 250 mL solution 0.2 M $FeSO_4$, under gaseous N_2 flow. The experiment was performed up to 6 h on a water bath heated by a combined hot-plate magnetic-stirrer device (Biosan, Riga, Latvia) at 30 °C and mixed at 1000 rpm to homogenize the FeS nanoparticles. FeS precipitate was divided in 11 parts (in 50 mL Eppendorf conical tubes) and FeS nanoparticles were centrifuged at 6000 rpm for 10

minutes and afterwards washed with N_2-flushed water. The FeS precipitate was frozen with liquid nitrogen and then freeze dried for about 48 h at about -80 °C. The dried powder of FeS was collected and stored in small Eppendorf plastic tubes of 2 mL sealed with teflon band until use. The FeS nanoparticles were characterized by determination of specific surface, X-Ray diffraction (XRD), Raman spectroscopy. Scanning electron microscopy (SEM), as well by Fourier-transform infrared spectroscopy (FTIR). The Raman and XRD peaks showed that mackinawite is the main crystalline phase of FeS nanoparticles, while the specific surface of the FeS was 32.58 m^2/g, which is similarly with the specific surface reported by (Liu et al., 2003) (see Supplementary Material).

2.3. Degradation experiments

The dehalogenation experiments were performed in 300 mL anaerobic bottles crimped by polytetrafluoroethylene (PTFE)-coated butyl septa. In the first experiment, the dehalogenation reaction was performed in duplicates by adding 165 mL buffer mixture solution K_2HPO_4 0.1 M/ KH_2PO_4 0.1 M (in a ratio of about 94 to 6) over 1.5 g FeS nanoparticles (final pH of 8.10 ± 0.04). The bottles were firstly flushed with nitrogen and then α-HCH was added from an acetone solution (3.43 mM α-HCH), to a theoretical concentration of approximatively 20.7 µM (see Tab.2). Also, a control bottle was prepared in duplicates by spiking 165 mL deionized water with α-HCH of the same concentration of 20.7 µM. In the first experiment, the dechlorination reaction was performed for 22 days in an incubator at 30 °C and 125 rpm. In the second experiment, the dehalogenation reaction was performed in three bottles by adding 165 mL deionized water over 1.5 g FeS nanoparticles (FeS concentration of 9.0 g/L). The pH of the three aquatic solutions was adjusted with 2-3 mL of 1M NaOH / 1M HCl to three final pH values: 2.4, 5.3 and 11.8. In this case also, the bottles were firstly purged with nitrogen and then α-HCH was added from the same acetone solution (3.43 mM α-HCH), to a concentration of approximatively 20 µM. In the 2nd experiment, the dechlorination reaction was performed for 32 days in an incubator at 30 °C and

125 rpm. The third experiment was carried out in 120 mL bottles screwed gas-tight by a butyl septum by mixing 1g of FeS nanoparticles with 110 mL N_2 flushed-water (FeS concentration of 9.0 g/L) and adjusting the pH to 9.9. In the 3rd experiment, the bottle was firstly purged with nitrogen and then spiked with α-HCH in acetone to a concentration in water of about 30 µM. In all three experiments, control bottles without FeS nanoparticles were used. At regular intervals, 14 mL aliquots of α-HCH solution were taken with syringes for extraction with 1 mL DCM that contains hexachlorobenzene (HCB) as internal standard, as previously described (Badea et al., 2009). The extraction and analysis of slurry samples of FeS nanoparticles was performed by ultrasonication and was similarly with the one of aliquots (see Supplementary Material).

2.4. Control experiment

In order to demonstrate that the decrease in concentration of α-HCH and the formation of the degradation products in the three experiments performed with FeS nanoparticles are attributable to the dehydrohalogenation processes that are taking place on the surface of FeS, an additional control experiment (experiment no. 4) was performed at three different pH values. The control experiments were performed using two 300 mL anaerobic bottles crimped by polytetrafluoroethylene (PTFE)-silicon septa. The first control bottle was preparing by dissolving $HgCl_2$ in 250 mL deionized water to a final concentration of 82 mg/L $HgCl_2$ in order to prevent any biodegradation of α-HCH, while the pH was adjusted to 7.0 by adding 0.4 mL 1M NaOH. In the second control bottle, the pH of 250 mL deionized water was adjusted to 9.99 using 2-3 mL of 1M NaOH / 1M HCl. In the third control bottle, the pH of 250 mL deionized water was adjusted to 11.7 with 0.9 mL 1M NaOH. In all three control bottles, 1 mL of solution 3.92 mM of α-HCH was added in both control bottles to final concentration of about 15.6 µM. Here too, 14 mL aliquots of α-HCH solution were taken with syringes for extraction with 1 mL DCM that contains hexachlorobenzene (HCB) as internal standard, the last sample for first and third control bottles (pH 7.0 and 11.7 respectively) being

166 taken after 17 days and the last one for the second control bottle (pH of 9.9) after 10 days. The
167 control experiment was performed up to 17 days in an incubator at 30 °C and 125 rpm.

168 *2.5. GC-MS analysis*

169 For the three degradation experiments with FeS, the GC-MS measurements were carried out on a
170 Varian 450 GC-240 MS (Varian, Inc, USA), equipped with an ion trap mass analyzer configurated
171 in positive electron ionization mode (70 eV). To identify and characterize the structure of the
172 degradation products, the ion trap mass analyzer was configured in scan mode. The samples (1 μL
173 DCM in volume) were injected at 260 °C into a split injector, with the split ratio adjusted to 20,
174 while the flow rate of carrier gas (helium) was 1 mL/min. The α-HCH and its degradation products
175 were separated on a CP-Sil 8 CB (8% phenyl polysilphenylene-siloxane) capillary column (30 m
176 × 0.25 m × 0.25 μm) using the following temperature program: 40 °C initial temperature (held for
177 3 min), 4 °C min^{-1} to 120 °C (0 min), 20 °C min^{-1} to 200 °C (0 min) and finally 10 °C min^{-1} to 280
178 °C (and held for 5 min).

179 In the experiment 4 (control experiment), the GC-MS measurements were carried out on a Perkin
180 Elmer Clarus 580 GC (Waltham, Massachusetts, USA), equipped with an Clarus SQ-8 quadrupole
181 mass analyzer configurated in positive electron ionization mode (70 eV). The samples (1 μL DCM
182 in volume) were injected into a split injector, with the split ratio adjusted to 10, while the flow rate
183 of carrier gas (helium) was 1 mL/min. The α-HCH and its degradation products were separated on
184 a DB5 MS (5% phenyl polysilphenylene-siloxane) capillary column (30 m × 0.25 m × 0.25 μm)
185 using the same temperature program as described in the paragraph above.

186 *2.6. GC-C-IRMS analysis*

187 The carbon isotope composition of α-HCH was analyzed using a gas chromatograph (Thermo
188 Trace 1310 GC, Thermo Scientific) coupled via a CONFLOW IV (Thermo Scientific, Germany)
189 to a Delta V Advantage mass spectrometer (Thermo Scientific, Germany), as described previously

(Zamane et al., 2020). The oxidation furnace of the interface (Thermo Scientific, Germany) containing Pt, Ni, and CuO was set to 1000 C° in order to completely combust α-HCH. The furnace was conditioned for 120 minutes with O_2 before each batch run of samples. The flow rate of carrier gas (helium) was 2.0 mL/min, while the injector was operated in split mode at 280°C. A DB-5MS GC column (60 m × 0.25 mm, 0.25 µm film thickness) was used for chromatographic separation of α-HCH from HCB. The temperature program of the GC oven was described previously (Badea et al., 2011) (see Supplementary Material).

2.7. Carbon stable isotope calculations

The carbon isotope signatures were reported in δ-notation (‰) relative to the Vienna Pee Dee Belemnite (V-PDB) (Coplen, 2011), as follows:

$$\delta^{13}C\,[‰] = \left(\frac{R_{sample} - R_{standard}}{R_{standard}}\right) \times 1000 \quad (1)$$

where the $^{13}C/^{12}C$ ratio of the sample (R_{sample}) is reported relative to the $^{13}C/^{12}C$ ratio of the VPDB-standard ($R_{standard}$).

The Rayleigh equation was used to quantify isotope fractionation upon degradation (equation 2):

$$\ln\left(\frac{R_t}{R_0}\right) = (\alpha - 1)\ln\left(\frac{C_t}{C_0}\right) \quad (2)$$

The C_0 and C_t and are the concentrations of the substrate at times 0 and t, while the R_0 and R_t are the $^{13}C/^{12}C$ ratios of the substrate at times 0 and t, respectively. The α is the isotope fractionation factor, and it can further used to calculate the isotope enrichment factor ε (equation 3):

$$\varepsilon = (\alpha - 1) \times 1000 \quad (3)$$

The error of the isotope enrichment factor was given as 95% confidence interval (CI) and determined using a regression analysis as described elsewhere (Elsner et al., 2007).

The apparent kinetic isotope effect (AKIE) was calculated using equation 4 according to (Elsner et al., 2005)

$$AKIE \approx \frac{1}{1+\left(\frac{n}{x}\cdot z\cdot\frac{\varepsilon}{1000}\right)} \quad (4)$$

where *x* is the number of reactive positions, *z* is the number of positions in intramolecular competition and *n* is the number of atoms of the molecule of a target element. The error propagation method was used to estimate uncertainty of the AKIE, as described elsewhere (Fischer et al., 2010).

3. Results and discussions

3.1. Dehalogenation of α-HCH by iron sulfide nanoparticles

α-HCH was dechlorinated in all degradation experiments at reaction times of up to 32 days. The main degradation products formed at all pH during dehalogenation were (Fig. 1, pathway (A)): 1,2,4-trichlorbenzene (1,2,4-TCB), 1,2-dichlorobenzene (1,2-DCB), benzene and, as intermediate, pentachlorocyclohexene (PCCH), tentatively identified by GC-MS by comparing its mass spectrum with those of the NIST library and with the previous degradation studies of α-HCH (Suar et al., 2005). (see Fig. S9, Supplementary Material). In the control bottles, no degradation products were detected. For example, in the experiment 1, no degradation products were detected and the isotope composition of α-HCH remained constant during the whole experiment indicating that the α-HCH from the control bottle is not biotically or abiotically transformed. Nevertheless, in the experiment 1, the concentration of α-HCH varied from 16.7 μM at the beginning of the experiment to 7.5 μM at the end of the experiment. This loss of α-HCH is probably attributable to the volatilization of α-HCH due to the low final volume of aquatic phase (about 54 mL) comparing with the initial one of 166 mL (with results in a large head-space volume), as well to the sorption processes. Small amounts of α-HCH might have been adsorbed onto the plastic syringes during sampling procedures. Also in the experiment no.4 without FeS nanoparticles, the evolution of α-

234 HCH concentration in the control bottles varied according to the initial pH values. In the control
235 bottle with the pH of 7.0, no degradation products were detected and the concentration of α-HCH
236 evolved from 15.6 μM at the beginning of the experiment to 16.6 μM after 17 days (at the end of
237 the experiment), showing no clear trend (see Fig.2). In control bottle with pH value of 9.9, the
238 concentration of α-HCH decreased from 15.4 μM at the beginning of the experiment to 11.9 μM
239 after 10 days (see Fig S7, Supplementary Material). In the control bottle with pH value of 9.9, the
240 pseudo-first-order rate constant was calculated to 0.090 d^{-1} which is slightly higher than the pseudo-
241 first-order rate constant of 0.069 d^{-1} recorded by (Ren et al., 2006) during alkaline hydrolysis of
242 α-HCH performed at pH 9.28 and 25°C, but was lower than the rate constant of 0.384 d^{-1} (0.0064
243 h^{-1}) recorded by (Zhang et al., 2014) during alkaline hydrolysis of α-HCH performed at pH 9.78.
244 In the control bottle with pH value of 11.7, the degradation rate was the fastest from all control
245 bottles, since the concentration of α-HCH decreased from 15.5 μM at the beginning of the
246 experiment to 0.3 μM after just one day (24 h), afterwards its concentration being bellow the
247 detection limit of the GC-MS method.

248 The above-mentioned degradation products (PCCH, 1,2,4-TCB, 1,2-DCB, benzene) showed that
249 the dehydrochlorination was the main degradation pathway of α-HCH by FeS. The proposed
250 degradation pathway from this study assumed a simultaneous elimination of two chlorine and two
251 hydrogen atoms from PCCH to produce 1,2,4-TCB, followed by a further reductive dechlorination
252 of 1,2,4-TCB to 1,2-DCB and finally to benzene ((Fig. 1, pathway (A)), in contrast with the
253 hydrolysis pathway recently proposed by (Kannath et al., 2019) (Fig. 1, pathway (B)) which
254 suggest an attack of the hydroxyl ion on the molecules of different HCHs isomers. The degradation
255 pathway from this study is also similar to a dehydrochlorination biotic pathways of α-HCH by
256 *Sphingomonas paucimobilis* B90A proposed by (Suar et al., 2005) and (Lal et al., 2010) (Fig. 1,
257 pathway (C)) , but the abiotic dehalogenation reaction is going beyond 1,2,4-TCB with the
258 formation of 1,2-dichlorobenzene and benzene as new degradation products.

The proposed degradation pathway was supported by the absence of monochlorobenzene (MCB) as degradation product. The vicinal dehaloelimination (vicinal reductive dechlorination) of α-HCH by FeS nanoparticles might be just a minor degradation pathway. In contrast with the previous studies (Badea et al., 2011), as the key intermediate of such pathway, the 3,4,5,6-tetrachloro-1-cyclohexene (TCCH, Fig. 1 pathway (D)) was detected just in the FeS slurry samples (see Fig. S13, Supplementary Material), but not in the aquatic ones. Since no reference standards of PCCH and TCCH were available for calibration, the concentrations (in μM) were calculated only for the 1,2,4-TCB, 1,2-DCB and benzene. The trend of degradation products in aquatic samples was influenced by the rate of α-HCH dechlorination which was influenced by the pH on the solutions. The ratio between final concentration of 1,2,4-TCB to 1,2-DCB varied from about 7.3 at pH 8.1 to about 32.9 at pH 11.8, indicating that the formation of 1,2-DCB by reductive dechlorination of 1,2,4-TCB is favored in heterogenous systems at more neutral pH, as previously found (Mackenzie et al., 2005). α-HCH was degraded completely in aquatic solutions only at pH 11.8 after 11 days, his concentration decreasing from 5.0 μM at the beginning of the 2nd experiment to 0.003 μM after 3 days and to further 0.002 μM after 7 days, afterwards the α-HCH being below the detection limit of the GC-MS method. In comparison, in the same 2nd experiment, the α-HCH concentrations decreased from 8.7 μM at the beginning of the experiment to 5.0 μM (pH 5.3) and respectively from 8.4 μM to 5.6 μM (pH 2.4), after 32 days of degradation, showing a high influence of pH on the degradation rate of α-HCH (see Fig. 2). In the 1st experiment, performed at pH 8.1, the α-HCH concentration decreased from 9.0 ± 0.4 μM at the beginning of the experiment to 5.6 ± 0.1 μM, after 22 days, at the end of the experiment. (Fig. 2). In the 3rd experiment performed at pH 9.9, the apparent degradation rate of α-HCH was slightly slower comparing with the one at pH 11.8 (see the apparent rate constants from Tab. 1), the α-HCH concentration decreasing from 5.9 μM at the beginning of the experiment to 0.5 μM after 4 days and to 0.041 μM after 19 days, at the end of the experiment (Fig. 2). This influence of pH on the degradation rate was also observed by (Liu et al.,

2003) in the degradation study of γ-HCH isomer with FeS nanoparticles. In order to explain the influence of pH on degradation rate, (Butler and Hayes, 1998) suggested that the dehalogenation rate of chlorinated chemicals (i.e. hexachloroethane) at alkaline pH is higher comparing with the reaction rate at acidic pH, possible due to deprotonation of species from the surface of FeS (deprotonated species have a higher reactivity). Nevertheless, in our study, the "apparent" degradation rate of α-HCH might be overestimated and might differ from the "true" degradation rate due to the sorption of α-HCH on the surface of FeS nanoparticles. This assumption is supported by the above-mentioned values of measured aquatic concentrations at the beginning of the experiments 1, 2 and 3 which were all lower than the initial spiked aquatic concentrations of about 20 µM (respectively around 30 µM for 3rd experiment). For the experiment 1, only about 43.7 % (1.49 µmoles out of 3.44 µmoles) of the total quantity of spiked α-HCH was detected in first aquatic samples taken, the rest being adsorbed on surface of FeS nanoparticles. To quantitively determine the influence of pH on the degradation rate, the kinetics of α-HCH degradation by FeS was assessed by considering the dehalogenation reaction to follow a pseudo first order kinetic. Therefore, the apparent rate constants (k_a) for the dehalogenation of α-HCH were calculated at different pH values (Tab.1), in the three different experiments, having all of them the same level of FeS to liquid ratio (the same FeS concentration of about 9 g/L) in the respective bottles. In the acidic pH domain, the apparent rate constant value showed only a small increase from 0.009 d^{-1} at pH 2.4 to 0.014 d^{-1} at pH 5.3 (both in 2nd experiment). In the alkaline pH domain, the apparent rate constants increased from 0.018 ± 0.002 d^{-1} at pH 8.1 (1st experiment) to 0.25 d^{-1} at pH 9.9 (3rd experiment), while the highest apparent rate constant of 1.1 d^{-1} was recorded at pH 11.8 (2nd experiment). The value of apparent rate constant recorded at pH 11.8 (1.1 d^{-1}) was higher than the rate constant of 0.384 d^{-1} (0.0064 h^{-1}) recorded by (Zhang et al., 2014) during alkaline hydrolysis of α-HCH performed at pH 9.78. These increases in k_a values clearly showed that the apparent rate constants during dehalogenation of α-HCH by FeS increased with pH, which was also shown by (Liu et al., 2003)

for γ-HCH isomer. By comparing the apparent rate constant of 0.25 d^{-1} recorded during dehalogenation of α-HCH by FeS at pH 9.9 (3rd experiment), with the pseudo-first-order rate constant of 0.090 d^{-1} recorded during hydrolysis of α-HCH in the control bottle with same pH value of 9.9 (4th experiment), it can be concluded that the kinetics of α-HCH dehalogenation of by FeS at moderate alkaline pH values (up to 10) is different from the one of hydrolysis. Nevertheless, at very high pH values (higher than 10) the contribution of hydrolysis can became significant.

At the end the of experiment 1, the concentrations of α-HCH and of its main degradation products in the FeS slurry were: 0.840 ± 0.008 µmol/g for α-HCH, 0.008 ± 0.003 µmol/g for 1,2,4-TCB and 0.0009 ± 0.0004 µmol/g for 1,2-DCB, respectively (see Tab. 2). These values can be used to calculate a mass balance. In this respect, the number of moles from the FeS slurry for α-HCH (1.26 µmol), 1,2,4-TCB (0.012 µmol) and 1,2-DCB (0.0013 µmol) must be considered, taking into account the quantity of FeS nanoparticles (1.5 g). As in many degradation studies, the mass balance is taking into account firstly the final aquatic concentrations of the compounds which were ranged between 5.6 ± 0.1 µM for α-HCH (the number of moles of α-HCH was 0.3024 µmol), 0.844 ± 0.045 µM for 1,2,4-TCB (0.0455 µmol) and 0.115 ± 0.098 µM for DCB (0.0062 µmol), respectively (see Tab. 2). The number of moles for each compound were calculated taking into account the final volume of aquatic phase (about 54 mL) at the end of the experiment. Nevertheless, due to complex nature of the degradation experiments with FeS nanoparticles (Li et al., 2016), the mass balance must include also the amounts of α-HCH, 1,2,4-TCB and 1,2-DCB removed from the degradation bottles by sampling. The number of moles removed from the bottles by sampling were: 0.7508 µmol for α-HCH, 0.0360 µmol for 1,2,4-TCB and 0.0050 µmol for 1,2-DCB, and these values were calculated individually for every compound as sum of numbers of moles of removed in every sampling point (with the volume of 14 mL), taking into account that 1,2,4-TCB and 1,2-DCB were measured only in the last seven, respectively five sampling point (out of eight). The total sum of these values at the end of experiment 1 was 2.42 µmol which means a recovery

334 of 70.4 % in the mass balance, comparing with the initially spiked amount of 3.44 µmol of α-HCH
335 (the spiked concentration of α-HCH was 20.7 µM at an initial volume of 166 mL). This slightly
336 difference between the numbers of moles at the beginning and at the end of experiment 1 is
337 probably due to transformation of α-HCH in the intermediates PCCH and TCCH, as well to the
338 more volatile nature of 1,2,4-TCB and 1,2-DCB.

339 *3.2. Carbon isotope fractionation in the course of α-HCH dehalogenation by FeS*

340 In the first degradation experiment performed at pHs 8.1 and 11.8, the carbon isotope composition
341 of α-HCH changed during dehalogenation. Since a pH value of 8.1 is of more relevance for real
342 environmental conditions (compared to pH of 11.8 where hydrolysis is fast), the isotope
343 fractionation of α-HCH was assessed only at pH value of 8.1. Note that Ren et al (2005) obtained
344 a half-life time of 74 days for hydrolysis of α-HCH at pH 8.3. The $\delta^{13}C$ values of $\delta^{13}C$ of the
345 internal standard HCB stayed constant. The carbon isotope composition of α-HCH increased from
346 -25.8 ± 0.6 ‰ to -23.1 ± 0.4 ‰, whereas the α-HCH concentrations decreased from 9.0 ± 0.4 µM
347 to 5.6 ± 0.1 µM (Fig. 3A). 1,2,4-trichlorbenzene (1,2,4-TCB) and 1,2-dichlorobenzene (1,2-DCB)
348 were detected after one and respectively 6 days of degradation, in concentrations of 0.014 ± 0.001
349 µM for 1,2,4-TCB and 0.019 µM for 1,2-DCB, respectively. At the end of the experiment (after 22
350 days), the concentrations increased to 0.844 ± 0.045 µM (1,2,4-TCB) and to 0.115 ± 0.098 (1,2-
351 DCB) (Fig. 3B), while β-PCCH was detected only as traces. For this experiment, the concentrations
352 of 1,2,4-TCB, 1,2-DCB and β-PCCH were smaller than the linearity range of the GC-C-IRMS
353 instrument and thus their isotope compositions could not be determined. Nevertheless, in the 2nd
354 experiment, the evolution of concentration of 1,2,4-TCB in the bottle with the pH of 11.8, allowed
355 a determination of isotope signature of 1,2,4-TCB during its formation, as well the elucidation of
356 trends of 1,2,4-TCB, 1,2-DCB and benzene concentrations during dehalogenation of α-HCH by
357 FeS performed at more alkaline pHs. In the bottle with the pH of 11.8, the first changes in the
358 concentrations of 1,2,4-TCB, and 1,2-DCB and benzene appeared after about 40 minutes, when

359 the 1st sample was taken (Fig. 4A and 4B), due to the fast dehalogenation reaction. After about 40
360 minutes, the recorded concentration of 1,2,4-TCB was 8.5 μM (the first day of the experiment) and
361 increased to a maximum of 15.7 μM after 3 days of degradation. Afterwards its concentration
362 decreased to 7.9 μM at the end of the experiment, whereas the isotope composition of 1,2,4-TCB
363 decreased from -31.2 ± 0.3 ‰ after 3 days of degradation (lighter than the initial isotope
364 composition of α-HCH) to -25.2 ± 0.1 ‰ after 32 days of degradation (Fig. 4A).

365 The first recorded concentration of 1,2-DCB was 0.31 μM at 40 minutes (in the 1st day of the
366 experiment), then it increased to a maximum of 0.45 μM after 5 days of degradation, and afterwards
367 decreased to 0.24 μM, after 32 days of degradation (Fig. 4B). The concentration of benzene
368 increased from 0.08 μM after 3 days of degradation to 0.12 μM, after 32 days of degradation (data
369 not shown). These changes in concentration of α-HCH degradation products showed that reaction
370 rates of 1,2-DCB and respectively benzene are slower comparing with the initial reaction of α-
371 HCH to 1,2,4-TCB. Here too, the concentrations of 1,2-DCB and PCCH and benzene were smaller
372 than the linearity range of the GC-C-IRMS instrument and thus their isotope compositions could
373 not be determined.

374 *3.3. Quantitative assessment of isotope fractionation during dehalogenation of α-HCH by FeS*

375 The enrichment factor (ε_C) of α-HCH dechlorination in the 2nd experiment was calculated using
376 according to the Rayleigh equation (equation 2) and gave a value of ε_C = -4.7 ± 1.3 ‰, while the
377 correlation coefficients (R^2) was 0.94 (Fig. 5). This ε_C is higher (in absolute value) than the values
378 of −1.6 ± 0.3 ‰ and −1.0 ± 0.2‰ recorded for *S. indicum strain B90A* and *S. japonicum strain*
379 *UT26*, respectively, for the dehydrochlorination pathways recorded by (Bashir et al., 2013) during
380 aerobic biodegradation of bulk α-HCH, but lower than the ε_C of -7.6 ± 0.4‰ recorded by (Zhang
381 et al., 2014) during dehydrochlorination of bulk α-HCH induced by alkaline hydrolysis (pH 9.78).
382 As demonstrated by (Zhang et al., 2014), the carbon isotope enrichment factors of individual
383 enantiomers ($\varepsilon_{C(+)}$, $\varepsilon_{C(-)}$) of α-HCH upon chemical transformation were statistically identical with

each other and they fall within the respective ε_C of bulk α-HCH within a 95% confidence interval, therefore an enantioselective stable isotope analysis (ESIA) of α-HCH was not investigated in this paper.

Considering dehydrohalogenation as the dominant degradation pathway of α-HCH by FeS, then the recorded values of εC = -4.7 ± 1.3 ‰ from this study is also lower than the enrichment factors (ε*C*) of γ-HCH recorded recently (Schilling et al., 2019) during dehydrohalogenation of γ-HCH by lindane dehydrochlorinases enzymes LinA1 (–8.1 ± 0.3 ‰) and LinA2 (–8.3 ± 0.2 ‰). Nevertheless, if the vicinal dihaloelimination is taken into consideration as possible degradation pathway of α-HCH by FeS (albeit a minor one), then the recorded εC is similar with the εC of −4.9 ± 0.1‰ previously reported by (Zhang et al., 2014) during dihaloelimination of α-HCH by Fe nanoparticles and with the εC of -3.7 ± 0.8 ‰ reported by (Badea et al., 2011) during dihaloelimination pathway during anaerobic biodegradation of α-HCH by *C. pasteurianum*. The recorded εC = -4.7 ± 1.3 ‰ from this study is also similar to the εC values of −4.2 ± 0.4‰ and−3.6 ± 0.4‰ recorded by (Liu et al., 2020b) for α-HCH and γ-HCH, respectively, during anaerobic biodegradation by an enrichment culture. Comparing with the εC from this study, using the same enrichment culture, (Liu et al., 2020b) recorded a lower εC of −1.9 ± 0.3‰ for β-HCH, but a higher one of 6.4 ± 0.7‰ for δ-HCH. Regarding the isotope fractionation appeared during the abiotic degradation of organohalides by FeS, (Koster van Groos et al., 2018) recorded an isotope enrichment factor of −19.3 ± 2.4 ‰ during reductive debromination of the 1,2-dibromoethane by FeS.

For a more comprehensive elucidation of the reaction pathway, the apparent kinetic isotope effect ($AKIE_C$) (Elsner et al., 2005) was assessed assuming an elimination reaction with concerted bond cleavage at one axial H/Cl pair of α-HCH to form pentachlorocyclohexene (PCCH). In this case, two carbons with axial chlorine hydrogen pairs (x = 2) with two indistinguishable positions (z = 2) were considered in the calculation of $AKIE_C$, while α-HCH has 6 carbon atoms (n=6). The resulting

409 $AKIE_C$, 1.029 ± 0.008, is slightly lower compared to the $AKIE_C$ value of 1.035 ± 0.004 calculated
410 by (Liu et al., 2019) for LinA1 but higher to the $AKIE_C$ value of 1.011 ± 0.001 calculated for
411 LinA2, during a study involving dehydrochlorination of α-HCH by Sphingobium indicum Strain
412 B90A and by corresponding enzymes. The resulting $AKIE_C$, 1.029 ± 0.008, is also lower than the
413 value of 1.048 ± 0.003 recorded by (Zhang et al., 2014) during alkaline hydrolysis of α-HCH.
414 However, if we assume that two C-Cl bonds are stepwise and reductively cleaved during the
415 reaction of α-HCH to TCCH, we have to consider that a two-electron transfers to the α-HCH
416 molecule for dichloroelimination can take place stepwise or in a concerted mode (Tobiszewski and
417 Namieśnik, 2012). The calculated $AKIE_C$ values of 1.029 ± 0.008 (for a stepwise electron transfer)
418 and of 1.014 ±0.004 (for a two-electron transfer) are similar to the values of 1.026 ± 0.003 (for a
419 stepwise electron transfer) and of 1.013 ± 0.001 recorded by (Liu et al., 2020b) during anaerobic
420 biodegradation of α-HCH by an enrichment culture. The recorded $AKIE_C$ values from this study
421 are also similar to the values of 1.030 ± 0.0006 (for a stepwise electron transfer) and of
422 1.015 ± 0.0003 (for a two-electron transfer) recorded by (Zhang et al., 2014), during
423 dihaloelimination of α-HCH by Fe nanoparticles. As suggested by (Butler and Hayes, 1998), the
424 predominance of dehydrochlorination in the degradation of α-HCH by FeS from this study, instead
425 of vicinal dihaloelimination, might be attributable to the FeS surface hydrolysis and this creates
426 heterogeneously vicinal species (that can be either protonated or deprotonated depending on pH).
427 The heterogeneously vicinal species might favor the dehydrochlorination (elimination of HCl)
428 instead of vicinal dihaloelimination (elimination of two Cl atoms).

429 **4. Conclusions**

430 The results from this study clearly showed that carbon isotope fractionation occurs during
431 dechlorination of α-HCH by iron sulfide nanoparticles. Therefore, beside the biotic isotope
432 fractionation of HCH isomers induced by sulfate-reducing bacteria, the abiotic isotope
433 fractionation by biotic-formed FeS must be considered in anoxic sediments and aquifers

contaminated with HCH isomers, especially if the FeS is present in significant concentrations in those areas. Nevertheless, the degradation of HCH isomers has been studied only with abiotic FeS and therefore the extent of HCHs degradation in the field by biotic FeS is yet to be elucidated. These degradation products identified by GC-MS demonstrated that the dehydrochlorination is the main degradation pathway of the α-HCH by FeS, followed by formation of 1,2,4-TCB and by a novel degradation pathway which involves a to further reductive dechlorination of 1,2,4-TCB to 1,2-DCB and finally to benzene, without accumulation of monochlorobenzene. The results of the three degradation experiments clearly showed that the apparent first-order rate constants during dehalogenation of α-HCH by FeS increased with pH, which confirms the previous studies performed on the degradation of γ-HCH by FeS nanoparticles. Taking into account the novel reaction mechanism proposed in this study, the isotope enrichment factor obtained can be used as reference to assess and quantify the chemical and biological α-HCH transformation in the anoxic environments. The relevance of various dehalogenation reaction mechanisms of α-HCH by FeS are yet to be investigated using multi-element CSIA (i.e. hydrogen *vs*. carbon *vs*. chlorine) This approach can provide new perspectives to assess also the environmental fate of all HCH isomers, as well of other contaminants of emerging concern (CECs).

Acknowledgment

This work was performed within the projects PN 19110303 entitled "Advanced techniques for identifying sources of contamination and biochemical reactions in aquatic ecosystems" and PN 19 11 03 01 entitled "Studies on the obtaining and improvement of the acido-basic properties of the nanoporous catalytic materials for application in wastes valorization" financed by the Romanian Ministry of Research, Innovation and Digitalization, as well within the mobility project PN-III-P1-1.1-MC-2019-2019, financed by Executive Unit for Financing Higher Education, Research, Development and Innovation (UEFISCDI). The authors are grateful to Dr. Adriana Marinoiu and

458 chem. Elena Marin for specific area and pores distribution measurements and to chem. eng. Claudia
459 Sandru for pH measurements.
460
461

References

Ayala-Luis KB, Cooper NGA, Koch CB, Hansen HCB. Efficient Dechlorination of Carbon Tetrachloride by Hydrophobic Green Rust Intercalated with Dodecanoate Anions. Environmental Science & Technology 2012; 46: 3390-3397.

Badea SL, Vogt C, Gehre M, Fischer A, Danet AF, Richnow HH. Development of an enantiomer-specific stable carbon isotope analysis (ESIA) method for assessing the fate of alpha-hexachlorocyclohexane in the environment. Rapid Communications in Mass Spectrometry 2011; 25: 1363-1372.

Badea SL, Vogt C, Weber S, Danet AF, Richnow HH. Stable Isotope Fractionation of gamma-Hexachlorocyclohexane (Lindane) during Reductive Dechlorination by Two Strains of Sulfate-Reducing Bacteria. Environmental Science & Technology 2009; 43: 3155-3161.

Bae S, Lee W. Enhanced reductive degradation of carbon tetrachloride by biogenic vivianite and Fe(II). Geochimica et Cosmochimica Acta 2012; 85: 170-186.

Bashir S, Fischer A, Nijenhuis I, Richnow H-H. Enantioselective Carbon Stable Isotope Fractionation of Hexachlorocyclohexane during Aerobic Biodegradation by Sphingobium spp. Environmental Science & Technology 2013; 47: 11432-11439.

Butler EC, Chen LX, Darlington R. Transformation of Trichloroethylene to Predominantly Non-Regulated Products under Stimulated Sulfate Reducing Conditions. Ground Water Monitoring and Remediation 2013; 33: 52-60.

Butler EC, Hayes KF. Effects of Solution Composition and pH on the Reductive Dechlorination of Hexachloroethane by Iron Sulfide. Environmental Science & Technology 1998; 32: 1276-1284.

Coplen TB. Guidelines and recommended terms for expression of stable-isotope-ratio and gas-ratio measurement results. Rapid Communications in Mass Spectrometry 2011; 25: 2538-2560.

Elsner M, Imfeld G. Compound-specific isotope analysis (CSIA) of micropollutants in the environment — current developments and future challenges. Current Opinion in Biotechnology 2016; 41: 60-72.

Elsner M, McKelvie J, Lacrampe Couloume G, Sherwood Lollar B. Insight into Methyl tert-Butyl Ether (MTBE) Stable Isotope Fractionation from Abiotic Reference Experiments. Environmental Science & Technology 2007; 41: 5693-5700.

Elsner M, Zwank L, Hunkeler D, Schwarzenbach RP. A new concept linking observable stable isotope fractionation to transformation pathways of organic pollutants. Environmental Science & Technology 2005; 39: 6896-6916.

Fischer A, Weber S, Reineke AK, Hollender J, Richnow HH. Carbon and hydrogen isotope fractionation during anaerobic quinoline degradation. Chemosphere 2010; 81: 400-407.

He YT, Wilson JT, Su C, Wilkin RT. Review of Abiotic Degradation of Chlorinated Solvents by Reactive Iron Minerals in Aquifers. Groundwater Monitoring & Remediation 2015; 35: 57-75.

He YT, Wilson JT, Wilkin RT. Impact of iron sulfide transformation on trichloroethylene degradation. Geochimica et Cosmochimica Acta 2010; 74: 2025-2039.

Hunkeler D, R. U. Meckenstock, B. Sherwood Lollar, T. C. Schmidt and J. T. Wilson. A Guide for Assessing Biodegradation and Source Identification of Organic Ground Water Contaminants using Compound Specific Isotope Analysis (CSIA). Ada, Oklahoma 74820, US EPA, Office of Research and Development National Risk Management Research Laboratory,: EPA 600/R-08/148 2008.

Julien M, Gilbert A, Yamada K, Robins RJ, Höhener P, Yoshida N, et al. Expanded uncertainty associated with determination of isotope enrichment factors: Comparison of two point calculation and Rayleigh-plot. Talanta 2018; 176: 367-373.

Kannath S, Adamczyk P, Wu L, Richnow HH, Dybala-Defratyka A. Can Alkaline Hydrolysis of γ-HCH Serve as a Model Reaction to Study Its Aerobic Enzymatic Dehydrochlorination by LinA? International journal of molecular sciences 2019; 20: 5955.

512 Koster van Groos PG, Hatzinger PB, Streger SH, Vainberg S, Philp RP, Kuder T. Carbon Isotope
513 Fractionation of 1,2-Dibromoethane by Biological and Abiotic Processes. Environmental
514 Science & Technology 2018; 52: 3440-3448.
515 Kriegman-King MR, Reinhard M. Transformation of carbon tetrachloride in the presence of sulfide,
516 biotite, and vermiculite. Environmental Science & Technology 1992; 26: 2198-2206.
517 Kuder T, van Breukelen BM, Vanderford M, Philp P. 3D-CSIA: Carbon, Chlorine, and Hydrogen Isotope
518 Fractionation in Transformation of ICE to Ethene by a Dehalococcoides Culture.
519 Environmental Science & Technology 2013; 47: 9668-9677.
520 Lal R, Pandey G, Sharma P, Kumari K, Malhotra S, Pandey R, et al. Biochemistry of Microbial
521 Degradation of Hexachlorocyclohexane and Prospects for Bioremediation. Microbiology and
522 Molecular Biology Reviews 2010; 74: 58-+.
523 Lee W, Batchelor B. Abiotic Reductive Dechlorination of Chlorinated Ethylenes by Iron-Bearing Soil
524 Minerals. 1. Pyrite and Magnetite. Environmental Science & Technology 2002; 36: 5147-
525 5154.
526 Lesser LE, Johnson PC, Aravena R, Spinnler GE, Bruce CL, Salanitro JP. An Evaluation of Compound-
527 Specific Isotope Analyses for Assessing the Biodegradation of MTBE at Port Hueneme, CA.
528 Environmental Science & Technology 2008; 42: 6637-6643.
529 Li D, Peng Pa, Yu Z, Huang W, Zhong Y. Reductive transformation of hexabromocyclododecane
530 (HBCD) by FeS. Water Research 2016; 101: 195-202.
531 Liu X, Peng Pa, Fu J, Huang W. Effects of FeS on the Transformation Kinetics of γ-
532 Hexachlorocyclohexane. Environmental Science & Technology 2003; 37: 1822-1828.
533 Liu Y, Liu J, Renpenning J, Nijenhuis I, Richnow H-H. Dual C–Cl Isotope Analysis for Characterizing the
534 Reductive Dechlorination of α- and γ-Hexachlorocyclohexane by Two Dehalococcoides
535 mccartyi Strains and an Enrichment Culture. Environmental Science & Technology 2020a.
536 Liu Y, Wu L, Kohli P, Kumar R, Stryhanyuk H, Nijenhuis I, et al. Enantiomer and Carbon Isotope
537 Fractionation of α-Hexachlorocyclohexane by Sphingobium indicum Strain B90A and the
538 Corresponding Enzymes. Environmental Science & Technology 2019; 53: 8715-8724.
539 Liu YQ, Kummel S, Yao J, Nijenhuis I, Richnow HH. Dual C-Cl isotope analysis for characterizing the
540 anaerobic transformation of alpha, beta, gamma, and delta-hexachlorocyclohexane in
541 contaminated aquifers. Water Research 2020b; 184: 8.
542 Mackenzie K, Battke J, Kopinke FD. Catalytic effects of activated carbon on hydrolysis reactions of
543 chlorinated organic compounds: Part 1. γ-Hexachlorocyclohexane. Catalysis Today 2005;
544 102-103: 148-153.
545 Marco-Urrea E, Nijenhuis I, Adrian L. Transformation and Carbon Isotope Fractionation of Tetra- and
546 Trichloroethene to Trans-Dichloroethene by Dehalococcoides sp. Strain CBDB1.
547 Environmental Science & Technology 2011; 45: 1555-1562.
548 Muller TA, Kohler HPE. Chirality of pollutants - effects on metabolism and fate. Applied Microbiology
549 and Biotechnology 2004; 64: 300-316.
550 Nie Z, Wang N, Xia X, Xia J, Liu H, Zhou Y, et al. Biogenic FeS promotes dechlorination and thus de-
551 cytotoxity of trichloroethylene. Bioprocess and Biosystems Engineering 2020; 43: 1791-1800.
552 Ren M, Peng Pa, Huang W, Liu X. Kinetics of Base-Catalyzed Dehydrochlorination of
553 Hexachlorocyclohexanes: I. Homogeneous Systems. Journal of Environmental Quality 2006;
554 35: 880-888.
555 Schilling IE, Hess R, Bolotin J, Lal R, Hofstetter TB, Kohler HPE. Kinetic Isotope Effects of the
556 Enzymatic Transformation of gamma-Hexachlorocyclohexane by the Lindane
557 Dehydrochlorinase Variants LinA1 and LinA2. Environmental Science & Technology 2019; 53:
558 2353-2363.
559 Suar M, Hauser A, Poiger T, Buser H-R, Müller MD, Dogra C, et al. Enantioselective Transformation of
560 α-Hexachlorocyclohexane by the Dehydrochlorinases LinA1 and LinA2 from the Soil
561 Bacterium Sphingomonas paucimobilis B90A. Applied and Environmental
562 Microbiology 2005; 71: 8514-8518.

563 Tobiszewski M, Namieśnik J. Abiotic degradation of chlorinated ethanes and ethenes in water.
564 Environmental Science and Pollution Research 2012; 19: 1994-2006.
565 Vogt C, Dorer C, Musat F, Richnow H-H. Multi-element isotope fractionation concepts to characterize
566 the biodegradation of hydrocarbons — from enzymes to the environment. Current Opinion
567 in Biotechnology 2016; 41: 90-98.
568 Wacławek S, Silvestri D, Hrabák P, Padil VVT, Torres-Mendieta R, Wacławek M, et al. Chemical
569 oxidation and reduction of hexachlorocyclohexanes: A review. Water Research 2019; 162:
570 302-319.
571 Zamane S, Gori D, Höhener P. Multistep partitioning causes significant stable carbon and hydrogen
572 isotope effects during volatilization of toluene and propan-2-ol from unsaturated sandy
573 aquifer sediment. Chemosphere 2020; 251: 126345.
574 Zhang N, Bashir S, Qin J, Schindelka J, Fischer A, Nijenhuis I, et al. Compound specific stable isotope
575 analysis (CSIA) to characterize transformation mechanisms of α-hexachlorocyclohexane.
576 Journal of Hazardous Materials 2014; 280: 750-757.

577

578

579 **Tab. 1.** The values of the apparent rate constants for the dehalogenation of α-HCH calculated at

580 different pH values. The concentration of FeS was 9 g/L in all experiments.

Crt. No.	**pH value**	**Apparent rate constant (d^{-1})**	**Experiment**
1	2.4	0.009	2nd
2	5.3	0.014	2nd
3	8.1	0.018 ± 0.002	1st
4	9.9	0.253	3rd
5	11.8	1.098	2nd

581

582

583 **Tab. 2.** The concentration of α-HCH and of its major degradation products (1,2,4-TCB and 1,2-DCB) in aquatic samples and FeS slurry at the end of

584 the 1st experiment (after 22 days) (pH=11.8).

Theoretical spiked α-HCH concentration (µM)	**Final α-HCH aquatic concentration (µM)**	**Final α-HCH concentration in FeS slurry (µmol/g)**	**Final 1,2,4-TCB aquatic concentration (µM)**	**Final 1,2-DCB aquatic concentration (µM)**	**Aquatic ratio $C_{1,2,4\text{-}TCB}/C_{1,2\text{-}DCB}$**	**Final 1,2,4-TCB concentration in FeS slurry (µmol/g)**	**Final 1,2-DCB concentration in FeS slurry (µmol/g)**	**Final sum of α-HCH (µmol)**	**Final sum of 1,2,4-TCB (µmol)**	**Final sum of 1,2-DCB (µmol)**
20.7	5.6 ± 0.1	0.840 ± 0.008	0.844 ± 0.045	0.115 ± 0.098	7.3	0.008 ± 0.003	0.0009 ± 0.0004	2.3132	0.0935	0.0125

585

586

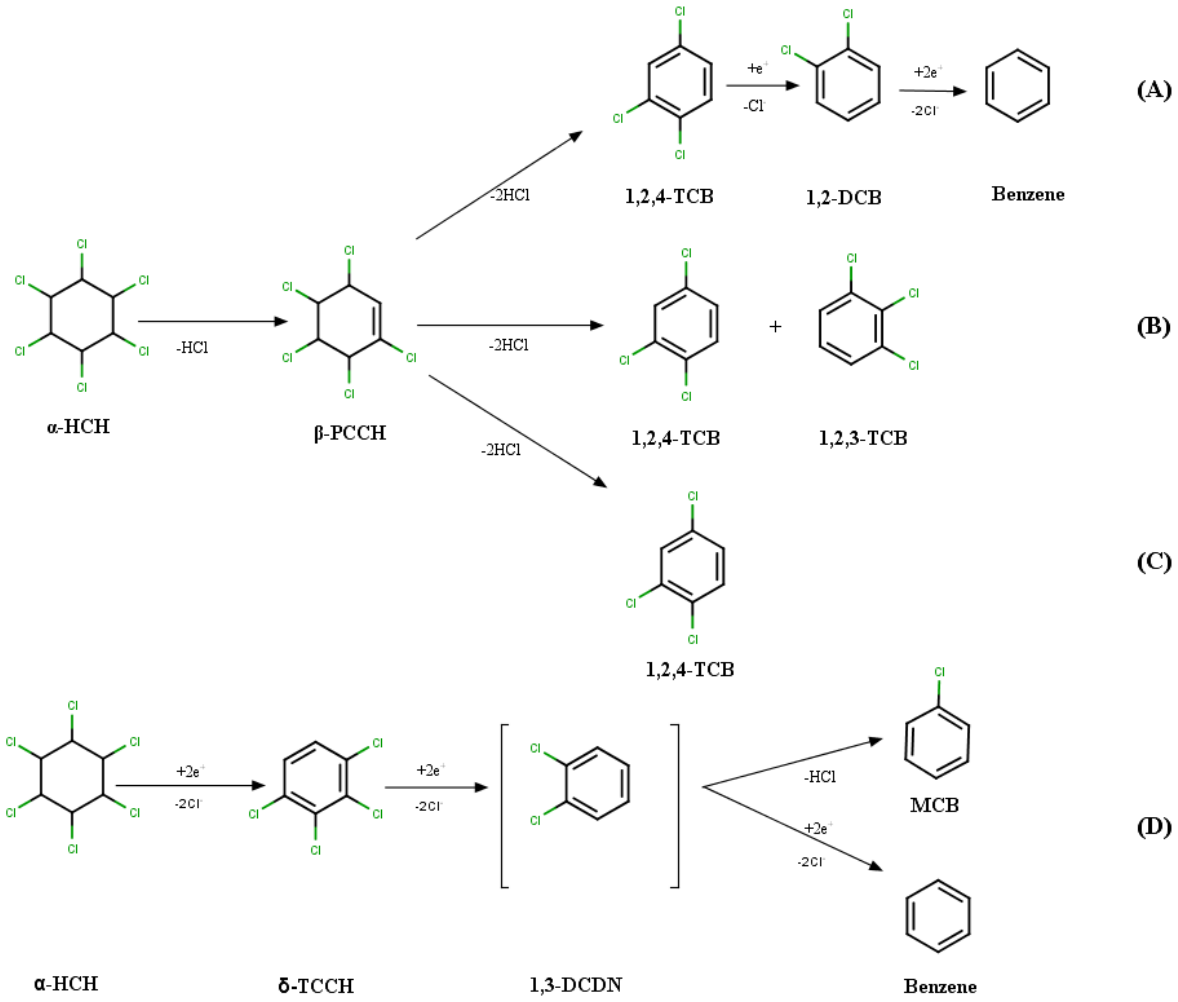

Fig. 1. The proposed pathway for the reductive dehalogenation of α-HCH with FeS nanoparticles from this study (A); Hydrolysis pathway proposed by (Kannath et al., 2019) (B); Biotic dehydrochlorination degradation pathway proposed by (Suar et al., 2005) (C); Biotic vicinal dihaloelimination pathway proposed by (Badea et al., 2011) (D).

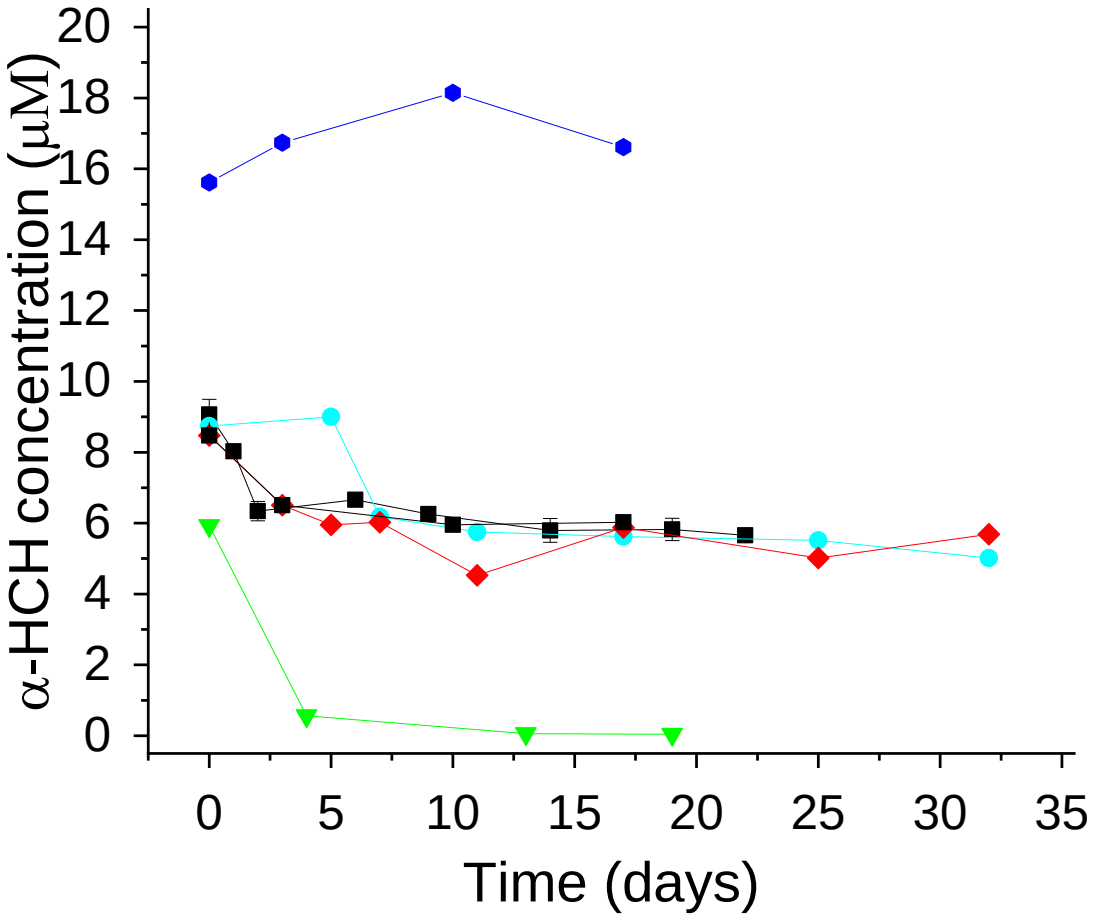

596

597 **Fig. 2.** The degradation curves of α-HCH by FeS at pH values: 8.1 (■) (experiment 1, black line);
598 2.4 (♦) and 5.3 (●) (experiment 2, cyan line); and 9.9 (experiment 3, green line) (▼), in three
599 different degradation experiments, as well the evolution of α-HCH concentration in the control
600 experiment (⬢) (experiment 4 without FeS, blue lines) at pH value of 7.0.

601

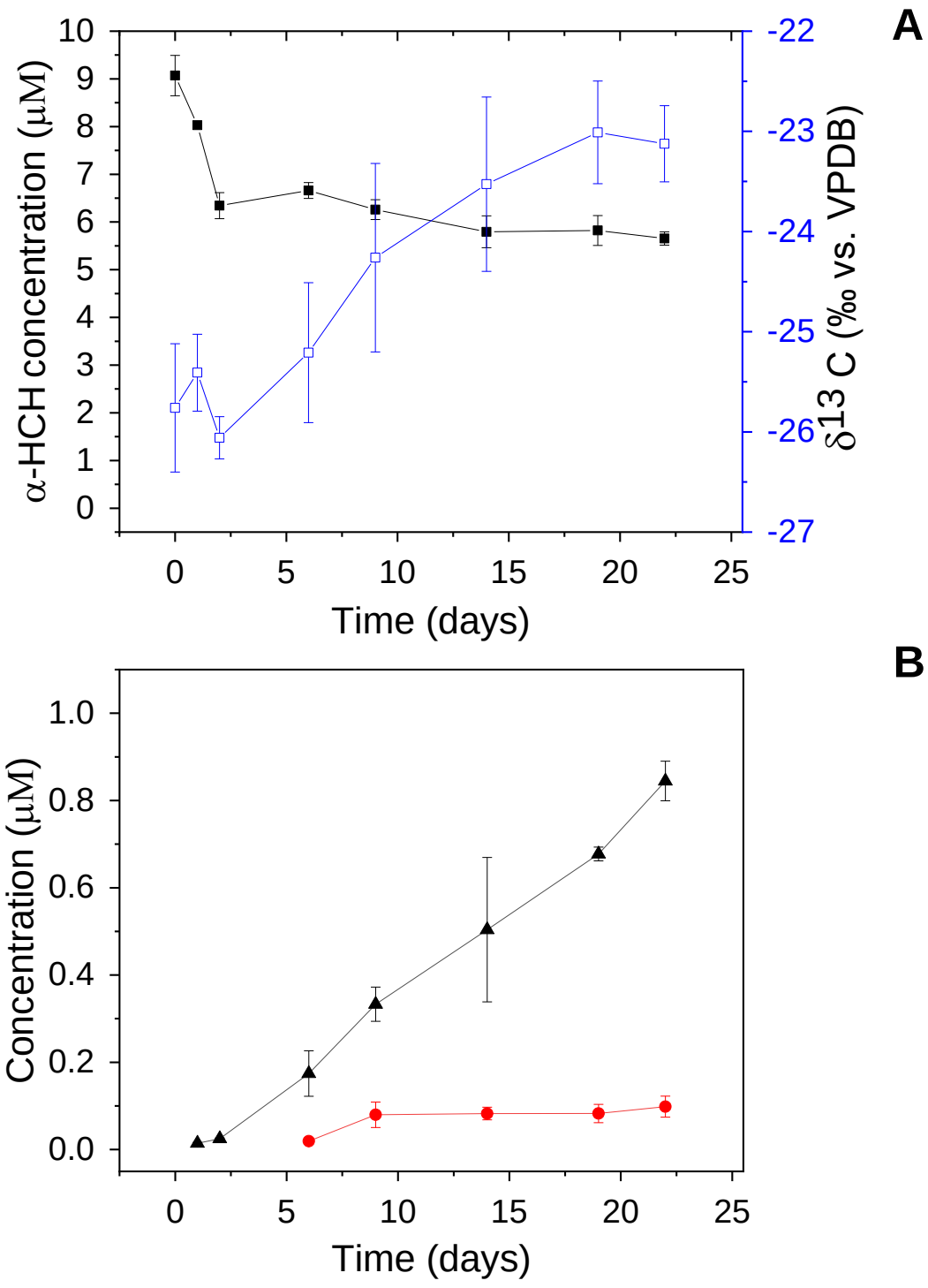

602

603 **Fig. 3.** Isotope signatures (□) vs. concentrations (■) of α-HCH during the 1st degradation
604 experiment by FeS at pH of 8.1 (A)**.** Formation of 1,2,4-TCB (▲) and 1,2-DCB **(●)** in the same
605 experiment with FeS (B). The error bars shown the standard deviation of the concentration values
606 between the two replicates, and the standard deviation of the isotope analysis, respectively.

607

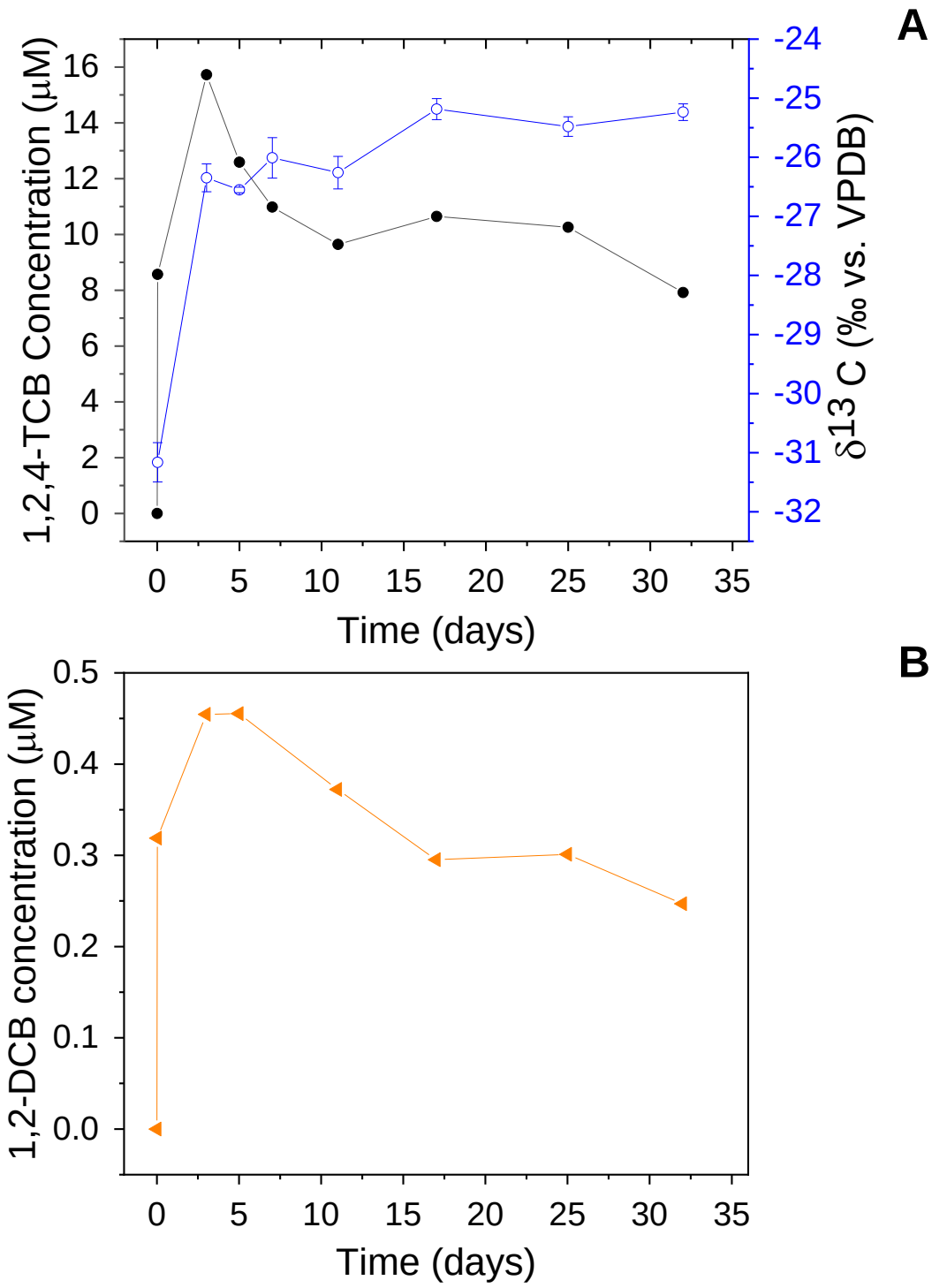

608

609 **Fig. 4.** Isotope signatures (○) vs. concentrations (●) of 1,2,4-TCB during the 2nd degradation

610 experiment by FeS at pH of 11.8 (A). Formation of 1,2-DCB (◀) in the same experiment (B).

611

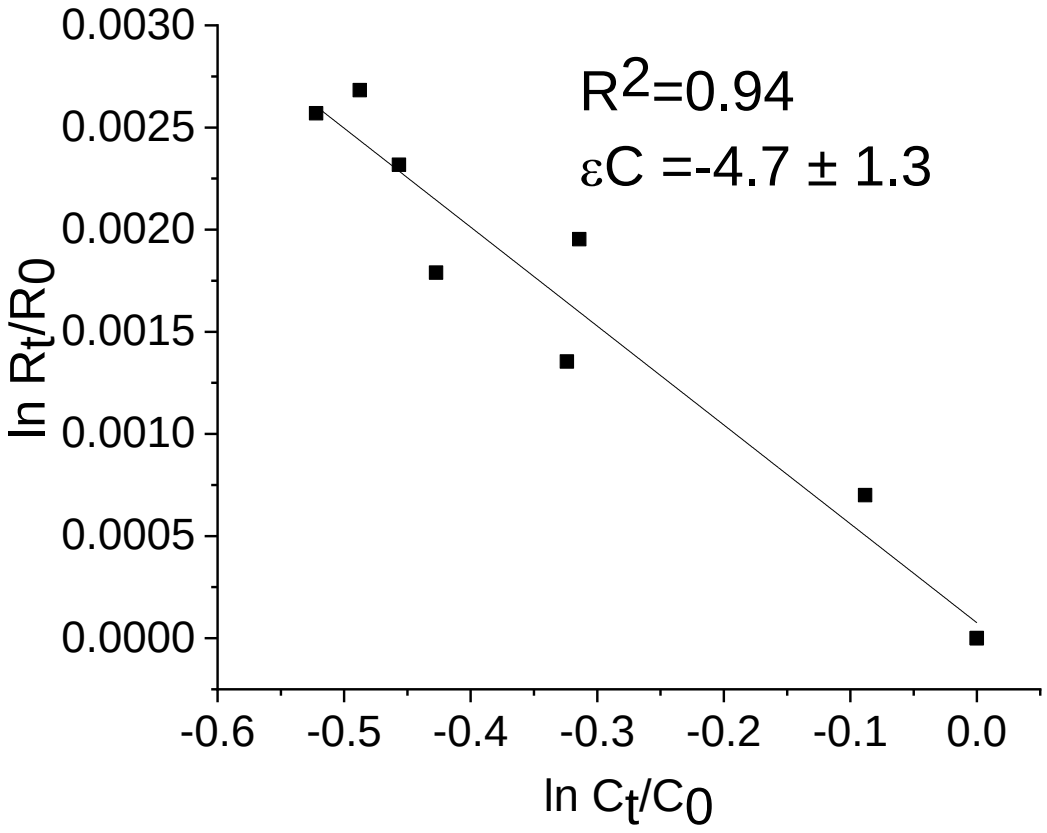

612

613 **Fig. 5.** Calculation of carbon isotope enrichment factor of α-HCH during dehalogenation by FeS

614 according to the Rayleigh model in experiment 1 (pH = 8.1).

615

616